Article

Not peer-reviewed version

Marine-Biomass-Derived Melanin–Chitosan Composites as Natural Black Hair Colorants: Charge Reversal and Electrostatic Deposition Mechanism

Toshihiko Matsuura * and Airi Nakajima

Posted Date: 31 March 2026

doi: 10.20944/preprints202603.2517.v1

Keywords: size-controlled ink particles (SIPs); cephalopod ink melanin; chitosan; natural hair coloration; electrostatic deposition; marine biomass

 doi:10.20944/preprints202603.2517.v1

Article

Marine-Biomass-Derived Melanin–Chitosan Composites as Natural Black Hair Colorants: Charge Reversal and Electrostatic Deposition Mechanism

Toshihiko Matsuura [1,*] and Airi Nakajima [2]

[1] Laboratory of Biotechnology & Bioengineering, Hokkaido University of Education, Hakodate, Japan

[2] Hokkaido SODA Co., Ltd., Tomakomai, Japan

* Correspondence: matsuura.toshihiko@h.hokkyodai.ac.jp

Abstract

Conventional oxidative hair dyes rely on aromatic amines, raising concerns about human health and environmental safety. This study reports a natural hair-coloring system using size-controlled ink particles (SIPs, ~170 nm in diameter) from cuttlefish ink and chitosan. Because both SIPs and hair surfaces carry negative charges near neutral pH, pristine SIPs exhibited poor deposition onto hair. Polyelectrolyte complexation with chitosan reversed the SIP surface charge under acidic conditions (maximum $\zeta \approx +41$ mV at pH 2.4), enabling electrostatic deposition onto hair fibers. Dynamic light scattering (DLS) revealed pH-responsive aggregation at pH 1.6–1.8 and redispersion at pH 2.8–4.3, while ultraviolet–visible (UV–Vis) spectra confirmed that the broadband absorption of melanin was preserved, consistent with predominantly noncovalent interactions. Scanning electron microscopy (SEM) showed a particle-based composite coating on hair fibers. An optimal SIP:chitosan weight ratio of 10:1 at pH ~4.7 yielded the darkest and most uniform coloration (L^* = 32.89, ΔE^*_{ab} = 55.89) without metallic mordants, achieving darker coloration than representative plant-based natural colorants reported in the literature. These results demonstrate a marine-biomass-derived approach to natural black hair coloration with strong darkening performance.

Keywords: size-controlled ink particles (SIPs); cephalopod ink melanin; chitosan; natural hair coloration; electrostatic deposition; marine biomass

1. Introduction

Hair coloring has become a widespread cosmetic practice around the world, and the global hair colorants market is projected to experience significant growth in the coming years [1,2]. However, conventional synthetic hair colorants typically contain aromatic amines such as *p*-phenylenediamine and related compounds, which raise serious health and environmental concerns [3–5]. These synthetic colorants have been associated with allergic reactions, skin irritation, and potential carcinogenic risks, prompting consumer demand for safer alternatives [6]. Consequently, there is a growing interest in developing natural, biocompatible hair colorants that can effectively color hair without causing adverse health effects.

Natural pigments derived from plants, such as henna, flavonoids, and curcuminoids, have been used as hair colorants for centuries [7,8]. However, these botanical colorants often have limitations including poor color fastness, a limited color range (predominantly reddish-brown tones), and prolonged application times. Furthermore, achieving black coloration, one of the most sought-after hair colors worldwide, remains particularly challenging using botanical colorants alone. This creates a significant opportunity to explore alternative natural black pigments that can overcome these limitations.

Melanin, the universal biological pigment responsible for the color of human hair, skin, and eyes [9], is an ideal candidate for natural hair colorants. It exhibits excellent biocompatibility, inherent

 doi:10.20944/preprints202603.2517.v1

black coloration, and UV-protective properties [10–14]. Melanin from cephalopod ink, such as that of cuttlefish and squid, has several advantages over other melanin sources. Cephalopod ink melanin is abundantly available as a by-product of the seafood industry, with global cephalopod catches exceeding 3 million tons annually [15,16]. It can be easily isolated at high purity and exists as well-defined nanoparticles that are suitable for cosmetic formulations [17]. Previous studies have established methods for isolating size-controlled ink particles (SIPs) from squid and cuttlefish, yielding monodisperse melanin particles with diameters ranging from 170 to 300 nm, whose physicochemical properties have been well characterized [18–23].

Despite these advantages, a critical challenge prevents the direct application of SIPs to hair. The surfaces of SIPs and human hair carry a negative charge at neutral pH due to the presence of carboxylic acid groups in melanin [24] and ionized amino acid residues in hair proteins [25,26]. This electrostatic repulsion inhibits SIP deposition onto hair surfaces, resulting in limited coloring performance. Previous research on melanin-protein interactions has demonstrated that electrostatic forces play a dominant role in binding behavior, with minimal interaction observed at neutral pH [27]. A similar trend was confirmed for SIPs by quartz crystal microbalance measurements, which showed negligible adsorption of the original SIPs onto negatively charged surfaces [28].

To overcome this electrostatic barrier, which remains a key obstacle to the practical application of melanin-based hair colorants, chitosan was selected as a cationic agent. Derived from crustacean shells, chitosan is a natural cationic polysaccharide that carries a positive charge in the acidic to neutral pH range [29]. The cationic nature of chitosan may reverse the surface charge of SIPs from negative to positive, thereby facilitating their deposition onto negatively charged hair surfaces. In addition, chitosan has been reported to exhibit favorable properties in hair-care formulations, including conditioning effects and reinforcement of hair fibers [30–32]. The combination of chitosan with SIPs may thus provide a synergistic effect, improving both coloration efficiency and hair quality.

This study tested the hypothesis that chitosan, a weak cationic polyelectrolyte, can induce charge reversal of SIPs via noncovalent complexation and thereby promote their electrostatic deposition onto hair. pH-dependent colloidal stability, surface charge regulation, preservation of melanin optical properties, surface coating morphology, and colorimetric performance were systematically evaluated as functions of the SIP:chitosan ratio and pH.

2. Materials and Methods

2.1. Materials

SIPs were isolated from the ink sacs of the common cuttlefish (*Sepia officinalis*) according to previously reported procedures [33,34]. The cuttlefish ink sacs were cut open with a dissecting knife, and the ink was extracted and collected through a sieve with 500 μm pore size. These samples were then mixed with a 0.1 M glycine-NaOH buffer solution (pH 10) containing protease (SD-AY10, Amano Enzyme Inc., Nagoya, Japan) at a protease dosage of 0.5 wt% relative to the dry weight of the ink. After shaking at 150 rpm and 50 °C for 24 h, the enzyme-treated samples were filtered through a 25 μm pore size sieve. Removal of impurities from the samples through ultrafiltration for 100 h at room temperature enabled purification and concentration of the SIPs. The purified SIPs were dispersed in ultrapure water (18.2 MΩ·cm) to obtain a stock suspension, and then stored at 4 °C. The samples were not frozen during purification or storage. The concentration of SIPs in the suspension was defined based on the dry mass, which was determined by drying suspension aliquots.

The chitosan solution (North Kiton V, 75 % deacetylated) was supplied by Hokkaido SODA Co., Ltd. (Hokkaido, Japan). The solvent was an acetic acid solution at a concentration of 1.2 wt%, and the concentration of chitosan was adjusted to be 1 wt% at pH 4.0. Citric acid and other reagents were purchased from FUJIFILM Wako Pure Chemical Corporation (Osaka, Japan) and used as received.

 doi:10.20944/preprints202603.2517.v1

2.2. Preparation of SIP–Chitosan Mixtures

SIP suspensions were mixed with the chitosan solution at weight ratios of 25:1, 10:1, 5:1, and 2:1 (SIP : chitosan). The mixtures were diluted with ultrapure water to adjust the concentration, and then stirred for 5 min. The final concentration of SIPs was adjusted to 0.03–7.0 g/L, depending on the experiment. The pH value of each mixture was adjusted by adding a 1 wt% aqueous citric acid solution to obtain the target pH values (pH 1.6–5.5).

2.3. Hair Coloring Test Procedure

Tresses of bleached human hair (100% white, 1 g, 10 cm) were obtained from STAFFS Co., Ltd. (Aichi, Japan). Prior to use, each hair tress was gently washed by hand using a commercial shampoo, and rinsed thoroughly with warm water at approximately 40 °C. The washed samples were then placed on paper towels and allowed to dry overnight at room temperature.

For the hair coloring experiments, the final concentration of the SIPs in the mixtures was 7.0 g/L. A volume of 1.4 mL of the mixture was applied to each tress of bleached human hair, spread evenly using gloved fingers. The treated hair tresses were covered with plastic wrap and incubated for 5 min to prevent drying during treatment. The tresses were then rinsed thoroughly with running water to remove excess mixture, placed on paper towels, and allowed to dry overnight at room temperature. All experiments were performed at least in triplicate.

2.4. Characterization

2.4.1. pH Measurement

The pH values of all samples were measured using a pH meter (SevenCompact s220, Mettler-Toledo AG, Greifensee, Switzerland) equipped with a glass electrode. The pH meter was calibrated with standard buffer solutions (pH 4.01, 6.86, and 9.18) before measurement. All pH measurements were performed at 25 °C.

2.4.2. Dynamic Light Scattering (DLS)

The hydrodynamic diameter was measured using a DLS analyzer (DLS-8000HAL, Otsuka Electronics Co., Ltd, Osaka, Japan) equipped with a solid-state blue laser (λ = 488 nm). To minimize dust contamination, all cuvettes were rinsed with ultrapure water and dried prior to use. All measurements were conducted at 25 °C. The reported values represent the average of three measurements.

2.4.3. Zeta Potential Measurement

The zeta potentials were measured using electrophoretic light scattering with a zeta potential analyzer (ELSZ-1000, Otsuka Electronics Co., Ltd, Osaka, Japan). Each sample was transferred into a flat cell, avoiding the introduction of air bubbles. The electrophoretic mobility was converted to zeta potential using the Smoluchowski relationship [35]. All experiments were performed at 25 °C. Each value represents the average of at least three independent measurements.

2.4.4. Ultraviolet–Visible (UV-Vis) Spectroscopy

UV-Vis spectra were recorded using a UV-Vis spectrophotometer (UV-1280, Shimadzu Corporation, Kyoto, Japan) over the wavelength range of 200–800 nm. A quartz cuvette with a path length of 1 cm was used. All measurements were performed at room temperature (approximately 25 °C).

 doi:10.20944/preprints202603.2517.v1

2.4.5. Scanning Electron Microscopy (SEM)

The surface morphology was observed using SEM (SU3500, Hitachi High-Tech Corporation, Tokyo, Japan, and JSM-6360LA, JEOL Ltd., Tokyo, Japan). The samples were mounted on aluminum stubs with double-sided carbon tape and sputter-coated with gold prior to observation. The acceleration voltages were set to 1.0-5.0 kV.

2.4.6. Color Measurement

The color of samples was evaluated using a spectrophotometer (Spectro1, Variable Inc., Chattanooga, TN, USA). The L^* value represents lightness on a scale from 0 (black) to 100 (white). A lower L^* value therefore corresponds to more effective darkening of the hair. The a^* and b^* values represent the red-green axis and the yellow-blue axis, respectively. The total color difference (ΔE^*_{ab}) was calculated using the following equation:

$$\Delta E^*_{ab} = \sqrt{(\Delta L^*)^2 + (\Delta a^*)^2 + (\Delta b^*)^2}, \quad (1)$$

where ΔL^*, Δa^*, and Δb^* are the differences in L^*, a^*, and b^* values between untreated and colored hair samples. Each measurement was repeated at least nine times. The results are expressed as the mean ± standard deviation (SD). All calculations were performed using Microsoft Excel (Microsoft 365).

3. Results

Figure 1 presents the variation in particle size of the SIPs and the SIP–chitosan mixture as a function of pH. The diameter of the original SIPs was approximately 170 nm at neutral pH, and remained relatively constant across the investigated pH range. This indicates that the SIPs were well dispersed and maintained colloidal stability without significant aggregation. This behavior is consistent with electrostatic stabilization of negatively charged SIPs (see ζ potentials in Figure 2). In contrast, the diameters of the SIP–chitosan mixture showed a pronounced pH dependence. Under strongly acidic conditions (pH 1.6–1.8), the apparent diameter increased dramatically to 610–680 nm, suggesting the formation of large aggregates or network-like structures comprising multiple SIPs bridged by chitosan. As the pH increased to around 2.8–4.3, the apparent diameters decreased to approximately 220–290 nm, indicating that the large aggregates disintegrated and a relatively stable dispersion was obtained. These values are slightly larger than those of the original SIPs, possibly due to chitosan adsorption on the SIP surface, but are far smaller than the aggregates observed under strongly acidic conditions. This pH-dependent transition from aggregation to stable dispersion is important for identifying the optimal processing conditions for hair coloring applications.

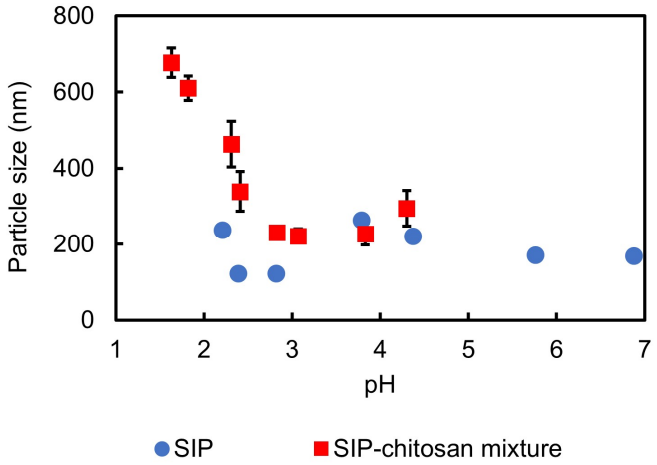

Figure 1. Hydrodynamic diameter of SIPs and SIP–chitosan mixtures as a function of pH, measured by DLS at a fixed SIP:chitosan weight ratio of 10:1.

 doi:10.20944/preprints202603.2517.v1

Figure 2 shows the pH dependence of the zeta potential of the SIPs and the SIP–chitosan mixture. The original SIPs exhibited negative zeta potentials over the entire pH range examined (pH 1.6–6.9). The zeta potential became more negative with increasing pH, changing from approximately −2 mV under acidic conditions to around −37 mV under near-neutral conditions. This behavior is attributed to the progressive deprotonation of carboxylic and phenolic functional groups present in melanin, resulting in an increasingly negatively charged particle surface. In contrast, the SIP–chitosan mixture showed positive zeta potentials under acidic conditions, with a maximum value of approximately +41 mV at pH 2.4. This indicates that cationic chitosan was successfully adsorbed onto the SIP surface, leading to charge reversal through electrostatic interactions between protonated amino groups of chitosan and negatively charged melanin sites.

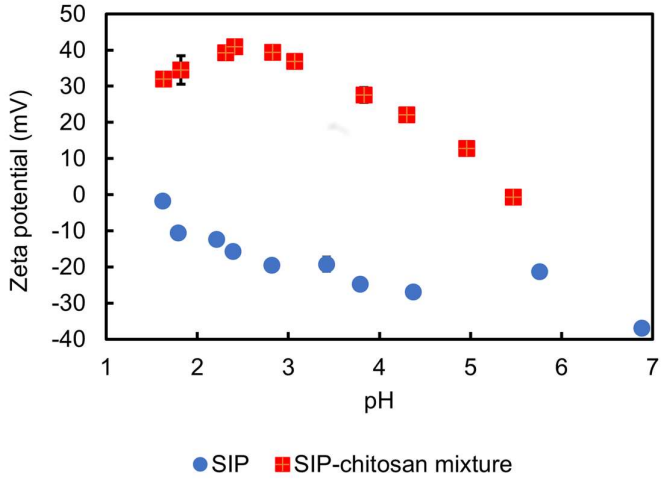

Figure 2. pH dependence of the zeta potential of SIPs and SIP–chitosan mixtures (SIP:chitosan = 10:1).

Figure 3 shows the UV–Vis absorption spectra of SIPs, chitosan, and SIP–chitosan mixtures under acidic conditions. The original SIPs exhibited a typical monotonic absorption profile, with strong absorbance in the UV region that gradually decreased toward the visible and near-infrared regions. This broadband, featureless spectrum is characteristic of melanin, reflecting its heterogeneous π-conjugated structure, which enables efficient light absorption over a wide wavelength range. In contrast, chitosan alone showed negligible absorption across the measured range, confirming that it does not contribute significantly to coloration.

The SIP–chitosan mixtures displayed spectral shapes nearly identical to those of the original SIPs regardless of the weight ratio (25:1 to 2:1). No new absorption bands or peak shifts were observed, suggesting that the interaction between SIPs and chitosan is predominantly electrostatic rather than involving substantial chemical modification of the melanin chromophores or alteration of their electronic structure. These results demonstrate that the mixture with chitosan preserves the intrinsic optical properties of melanin while enabling physicochemical modification of the particle surface, which is advantageous for maintaining natural coloration in the proposed hair-coloring system.

 doi:10.20944/preprints202603.2517.v1

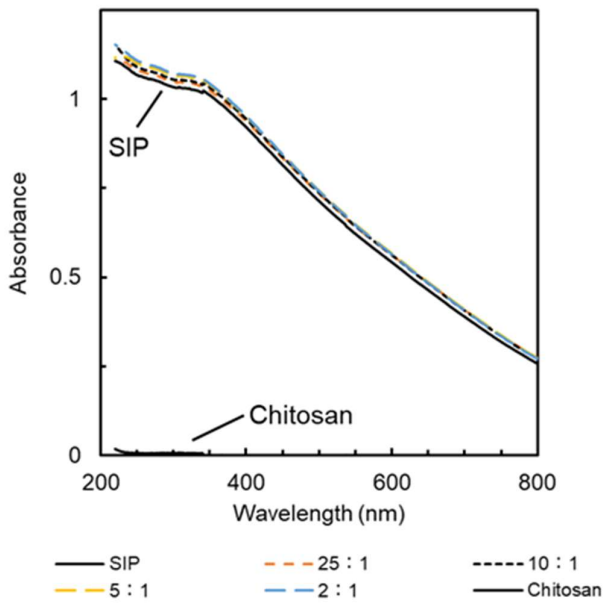

Figure 3. UV–Vis absorption spectra of SIPs, chitosan, and SIP–chitosan mixtures at different SIP:chitosan weight ratios.

Figure 4 shows SEM images of hair surfaces after coloration with the SIP–chitosan mixture. At lower magnification (left image), the treated hair fiber is covered with a relatively continuous coating layer along the hair shaft. The coated surface appears broadly and relatively uniformly distributed over the observed area, although some local surface irregularities remain visible. At higher magnification (right image), numerous spherical particles with submicrometer diameters are clearly observed on the hair surface. These particles are attributed to the deposited SIP–chitosan composites. In many regions, the particles are densely packed, whereas locally less densely covered areas and small aggregates are also observed. These observations provide morphological evidence of substantial deposition of the SIP–chitosan composites on the hair surface and support the interpretation that chitosan-mediated charge reversal promotes the electrostatic adsorption of SIPs onto negatively charged hair surfaces.

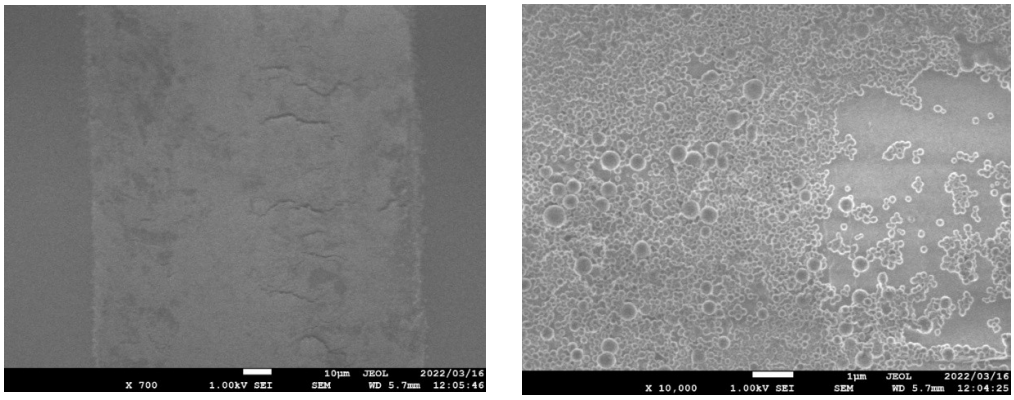

(**a**) (**b**)

Figure 4. SEM images of hair surfaces after coloration with the SIP–chitosan mixture (SIP:chitosan = 10:1, pH ~4.7). (**a**) Lower magnification; (**b**) Higher magnification.

Figure 5 shows the visual appearance of hair tresses treated with SIP–chitosan mixtures at different weight ratios under moderately acidic conditions (pH ~4.7). Distinct differences in

 doi:10.20944/preprints202603.2517.v1

coloration were observed depending on the SIP-to-chitosan weight ratio. The tresses treated with the original SIPs alone (without chitosan, 1:0) exhibited only slight coloration, confirming the expected electrostatic repulsion between negatively charged SIPs and hair surfaces. At a weight ratio of 25:1, coloration remained weak and uneven due to insufficient chitosan for effective charge reversal. Conversely, excess chitosan at weight ratios of 5:1 and 2:1 produced lighter and somewhat grayish tresses, likely because excess cationic polymer shielded the particle charge or promoted aggregation, reducing the effective SIP deposition density. The weight ratio of 10:1 yielded the most intense and uniform dark coloration, indicating that an optimal balance between charge reversal and dispersion stability was achieved at this weight ratio.

Figure 5. Photographs of bleached hair tresses after treatment with SIP – chitosan mixtures at different SIP:chitosan weight ratios under moderately acidic conditions (pH ~4.7).

Figure 6 shows the effect of pH on the coloration of hair tresses treated with SIP–chitosan mixtures at the weight ratio of 10:1. At the optimal weight ratio of 10:1 identified in Figure 5, a clear pH dependence was observed. Under near-neutral conditions (above pH 5), only weak coloration occurred, consistent with reduced protonation of chitosan and consequently weaker electrostatic attraction to the hair surface. Under strongly acidic conditions (below pH 2), coloration was also ineffective, which corresponds to the large-aggregate formation observed in DLS measurements (Figure 1). The most effective coloration was achieved at approximately pH 4.7, where moderate protonation of chitosan amino groups provided sufficient positive charge for efficient deposition while maintaining stable particle dispersion. Other weight ratios (25:1, 5:1, and 2:1) showed less effective coloration across all pH conditions, confirming that the coloring performance depends on the interplay between weight ratio and pH (Fig. S1 and Tables S1, S2, and S3).

Figure 6. Photographs of bleached hair tresses treated with the SIP–chitosan system at a fixed SIP:chitosan weight ratio of 10:1 at different pH values.

 doi:10.20944/preprints202603.2517.v1

Table 1 summarizes the colorimetric parameters (L^*, a^*, b^*, ΔL^*, and ΔE^*_{ab}) of hair tresses treated with SIP–chitosan mixtures at different weight ratios under moderately acidic conditions (pH ~4.7). These values quantitatively confirm the visual trends observed in Figure 5 and provide a detailed comparison of coloration across different weight ratios. Untreated bleached hair exhibited high lightness (L^* = 85.18 ± 2.19) with a pronounced yellowish tone (b^* = 18.62 ± 3.13). Among all mixtures tested, the 10:1 weight ratio produced the most pronounced darkening, yielding an L^* value of 32.89 ± 0.87 (ΔL^* = −52.29 ± 0.87) and the highest total color difference from untreated hair (ΔE^*_{ab} = 55.89 ± 0.85). The 10:1 weight ratio yielded the largest ΔL^* and ΔE^*_{ab} values among all colored samples, confirming its strong darkening performance. This mixture also brought both a^* (8.77 ± 0.33) and b^* (9.26 ± 0.22) closest to those of the natural black hair reference (a^* = 6.90; b^* = 3.48), indicating a simultaneous reduction in residual redness and yellowness. It is also worth noting that the 10:1 weight ratio exhibited the smallest standard deviations across all colorimetric parameters, suggesting superior uniformity of coloration compared with the other mixtures. In contrast, SIP alone (1:0) produced only a modest decrease in lightness (L^* = 70.77 ± 4.87) while increasing redness (a^* = 16.97 ± 2.60), and mixtures with excess chitosan (2:1) similarly showed limited darkening (L^* = 69.33 ± 2.27) with elevated a^* values (16.18 ± 3.24). The relationship between chitosan content and darkening efficiency was non-monotonic: increasing the chitosan proportion from 25:1 to 10:1 markedly enhanced coloration, whereas further increases to 5:1 and 2:1 diminished the effect. This trend suggests that an optimal SIP-to-chitosan balance is required to maximize deposition of the pigment onto the hair surface.

Table 1. Colorimetric parameters of hair tresses treated with SIP–chitosan mixtures at different weight ratios under moderately acidic conditions (pH ~4.7). Reference (natural black hair) is shown for comparison and was not included in the statistical comparison among treated bleached hair samples.

Weight ratio (SIP:chitosan)	L^*	a^*	b^*	ΔL^*	ΔE^*_{ab}
Untreated (bleached)	85.18 ± 2.19	26.12 ± 5.86	18.62 ± 3.13		
1:0 (SIP only)	70.77 ± 4.87	16.97 ± 2.60	14.46 ± 0.64	-14.41 ± 4.87	17.67 ± 5.19
25:1	57.70 ± 6.67	12.02 ± 2.87	12.27 ± 1.32	-27.48 ± 6.67	31.60 ± 7.03
10:1	32.89 ± 0.87	8.77 ± 0.33	9.26 ± 0.22	-52.29 ± 0.87	55.89 ± 0.85
5:1	51.56 ± 1.95	10.66 ± 0.91	11.70 ± 0.33	-33.62 ± 1.95	37.67 ± 1.68
2:1	69.33 ± 2.27	16.18 ± 3.24	11.09 ± 0.89	-15.85 ± 2.27	20.36 ± 2.75
Reference (natural black hair)	24.40 ± 1.17	6.90 ± 0.78	3.48 ± 0.46	-60.78 ± 1.17	65.52 ± 1.31

Overall, these results indicate that optimal hair coloration is achieved through a balance of weight ratio and pH. The 10:1 mixture at pH 4.7 produced the darkest and most uniform coloration, with color coordinates closest to those of the natural black hair reference, highlighting the importance of controlled deposition of SIPs on the hair surface. To further examine the pH dependence at the optimal weight ratio identified above, Table 2 summarizes the colorimetric parameters of hair tresses treated with the SIP–chitosan mixture at a fixed weight ratio of 10:1 over a pH range of 1.99–5.18. These results quantitatively support the optimal coloration observed at approximately pH 4.7 in Figure 6. Under strongly acidic conditions (pH 1.99–3.01), the hair tresses exhibited relatively high L^* values (66.61–67.84), indicating limited darkening. Correspondingly, the total color difference remained moderate, with ΔE^*_{ab} values ranging from 20.71 to 22.11. A gradual decrease in L^* was observed as the pH increased, reaching 60.21 ± 8.21 at pH 3.53. A pronounced change occurred around pH 4.68–4.88, where the L^* values dropped markedly to 32.96 ± 1.02 and 38.25 ± 1.32, respectively. At these pH values, the largest color differences were observed (ΔE^*_{ab} = 55.87 ± 0.95 and 50.30 ± 1.38), indicating the most effective coloration. At higher pH values (pH 5.08–5.18), the L^* values increased again (50.27–52.93), accompanied by a decrease in ΔE^*_{ab} (38.97–35.88), indicating reduced coloration intensity. These quantitative results confirm that the coloration efficiency of the

 doi:10.20944/preprints202603.2517.v1

SIP–chitosan mixture at a weight ratio of 10:1 is strongly dependent on pH, with the most effective darkening occurring in the moderately acidic region around pH 4.7.

Table 2. Effect of pH (1.99–5.18) on the colorimetric parameters of hair tresses treated with SIP–chitosan mixtures at a fixed weight ratio (SIP:chitosan = 10:1). Color differences were calculated relative to untreated bleached hair.

pH	L^*	a^*	b^*	ΔL^*	ΔE^*_{ab}
1.99	67.84 ± 3.30	15.98 ± 3.67	14.67 ± 1.10	-17.34 ± 3.30	20.71 ± 3.77
2.19	66.61 ± 7.81	15.16 ± 3.29	14.69 ± 1.00	-18.57 ± 7.81	22.11 ± 7.96
3.01	67.56 ± 8.37	14.31 ± 3.48	14.19 ± 1.04	-17.62 ± 8.37	22.08 ± 7.95
3.53	60.21 ± 8.21	12.90 ± 3.40	13.02 ± 1.40	-24.97 ± 8.21	29.22 ± 7.35
4.68	32.96 ± 1.02	8.58 ± 0.32	9.31 ± 0.21	-52.22 ± 1.02	55.87 ± 0.95
4.88	38.25 ± 1.32	9.75 ± 0.72	10.92 ± 0.21	-46.93 ± 1.32	50.30 ± 1.38
5.08	50.27 ± 2.08	10.40 ± 0.98	11.37 ± 0.51	-34.91 ± 2.08	38.97 ± 2.16
5.18	52.93 ± 4.02	11.75 ± 0.96	12.51 ± 0.63	-32.25 ± 4.02	35.88 ± 3.72

4. Discussion

4.1. Electrostatic Complexation Between SIPs and Chitosan

The zeta potential measurements demonstrated that the original SIPs were negatively charged throughout the examined pH range, whereas the SIP–chitosan mixtures exhibited charge reversal under acidic conditions. This behavior is attributed to protonation of the primary amino groups of chitosan, which have a pKa of approximately 6.5 [36]. Below this pKa, chitosan exists predominantly in the $-NH_3^+$ form, enabling strong electrostatic attraction to negatively charged SIPs. Such pH-dependent charge regulation is a characteristic feature of chitosan as a weak cationic polyelectrolyte [29]. The observed charge reversal therefore confirms the formation of a SIP–chitosan polyelectrolyte complex governed by Coulombic interactions rather than covalent modification.

4.2. pH-Controlled Aggregation and Dispersion Behavior

DLS revealed that SIP–chitosan mixtures aggregated under strongly acidic conditions but redispersed under moderately acidic conditions. At extremely low pH (below 2), two mechanisms likely contribute to the pronounced aggregation. First, the high charge density of fully protonated chitosan promotes interparticle bridging, in which highly charged polymer chains adsorb onto multiple particles simultaneously, leading to network-like aggregates [37]. Second, the protonation of carboxylic acid groups in melanin (pKa ~4–5 for 5,6-dihydroxyindole-2-carboxylic acid (DHICA) -type carboxyl groups [24]) reduces the negative surface charge density of SIPs, thereby weakening the electrostatic repulsion between particles and further facilitating aggregation. The combined effect of enhanced bridging by chitosan and diminished interparticle repulsion likely accounts for the large aggregates observed in this pH regime.

With increasing pH, partial deprotonation of chitosan reduced bridging while maintaining sufficient electrostatic attraction for surface complexation, producing stable hybrid particles. Such pH-responsive aggregation–dispersion transitions are well documented in chitosan-based colloidal systems and are governed by the balance between electrostatic attraction and steric stabilization [38].

4.3. Preservation of Melanin Optical Properties

UV–Vis spectroscopy showed that the broadband absorption profile characteristic of the SIPs remained unchanged after complexation with chitosan. This monotonic absorption profile, well documented for eumelanin [14], arises from chemical disorder in the π-conjugated structure. The absence of new spectral features indicates that the interaction between SIPs and chitosan is physical rather than chemical, suggesting that the chromophore structure responsible for coloration is

 doi:10.20944/preprints202603.2517.v1

preserved. This is advantageous for cosmetic applications, because the surface properties can be modified without altering the intrinsic optical functionality of the pigment.

4.4. Deposition Mechanism onto Hair Surfaces

SEM observations confirmed that SIP–chitosan composites formed a coating layer on hair surfaces. Human hair carries a net negative surface charge arising from ionized amino acid residues in keratin [26]. Because the isoelectric point of hair is around pH 3.6 [39], hair surfaces are negatively charged under mildly acidic conditions. Under these conditions, the charge-reversed SIP–chitosan composites can efficiently deposit onto hair surfaces through electrostatic attraction. Such electrostatic interactions between oppositely charged surfaces are widely recognized as a key mechanism governing the adsorption and deposition of colloidal particles onto solid substrates.

Unlike oxidative hair dyes, which rely on in situ chemical reactions within the cortex, this system functions through surface deposition of naturally derived pigments and thus represents a fundamentally different coloring mechanism. Because the colorant is deposited on the outermost surface of the hair shaft rather than being incorporated into the cortex, the color fastness upon repeated shampooing may be lower than that of oxidative dyes [6]. A systematic evaluation of color fastness under standardized washing protocols is currently underway.

4.5. Optimization of the SIP:Chitosan Weight Ratio and pH

Coloration experiments revealed that an intermediate weight ratio (10:1) provided the most effective coloration. Insufficient chitosan failed to induce adequate charge reversal, whereas excess chitosan promoted aggregation and reduced SIP deposition efficiency. Similar composition-dependent behavior has been reported for polymer–particle complexes, where optimal performance is achieved near charge-stoichiometric conditions [37,38]. The strong dependence on pH further confirms that controlled protonation of chitosan is essential: under near-neutral conditions, insufficient protonation weakened the electrostatic attraction to the hair surface, whereas under strongly acidic conditions, excessive protonation promoted large-aggregate formation. The optimal pH of approximately 4.7 represents a balance between these competing effects.

4.6. Implications for Marine Biomass–Derived Functional Materials

Because melanin extracted from cephalopod ink is an abundant marine byproduct and chitosan is derived from crustacean shells, their combination represents a sustainable strategy for valorizing marine biomass. The ability to tune surface charge, dispersion stability, and deposition behavior through simple pH control suggests a versatile platform for designing bio-derived functional coatings beyond hair-coloring applications.

4.7. Design Rule for Cosmetic Deposition

On the basis of ζ potential and DLS results, effective hair deposition requires (i) positive surface charge for electrostatic attraction and (ii) suppression of bridging-induced aggregation. Practically, this is achieved at pH ~4–5 with an intermediate SIP:chitosan ratio (10:1), where charge reversal is sufficient while colloidal stability is retained. To contextualize the coloring performance of the present system, the ΔE^*_{ab} values can be compared with those reported for other natural hair colorants applied to human hair. Sargsyan *et al*. reported ΔE values of 38.76–40.23 for a tannin–mordant system (matcha and iron(II)-lactate) on unpigmented Caucasian hair tresses, with the darkest shade reaching $L^* \approx 40.81$ [40]. Cui *et al*. evaluated four plant colorants with ferrous mordant on human bleached hair and reported ΔE values of 28.16 for henna, 31.42 for walnut husks, 35.22 for sappanwood, and 36.45 for Chinese gallnuts [41]. The ΔE^*_{ab} of 55.89 and L^* of 32.89 achieved by the SIP–chitosan system at the 10:1 weight ratio exceed the reported values under the respective experimental conditions, suggesting strong darkening performance relative to representative plant-based natural colorants. Importantly, the SIP–chitosan system achieves black coloration without the use of metallic mordants,

 doi:10.20944/preprints202603.2517.v1

which may pose concerns regarding metal accumulation on hair and potential photosensitization via Fenton-type reactions [41]. These practical and safety-related advantages highlight the potential of the marine-biomass-derived SIP–chitosan platform as a competitive alternative to existing natural hair colorants.

5. Conclusions

This study established a natural hair-coloring system based on SIPs derived from cuttlefish ink and chitosan. Electrostatic complexation with chitosan reversed the negative surface charge of SIPs, enabling their efficient deposition onto negatively charged hair surfaces without chemical oxidation. SEM confirmed the formation of a particle-based coating layer, providing direct morphological evidence for the electrostatic adsorption mechanism. The system exhibited pH-dependent colloidal behavior, where stable dispersions formed under moderately acidic conditions while preserving the intrinsic broadband optical absorption of melanin. Optimal coloration was achieved at a weight ratio of 10:1 around pH 4–5, yielding L^* = 32.89 and ΔE^*_{ab} = 55.89, which are larger than several values reported for plant-based natural colorants without metallic mordants. These findings establish a design rule for melanin-based hair colorants: effective deposition requires sufficient positive surface charge combined with suppression of bridging-induced aggregation, both achievable through pH control and an optimized SIP:chitosan ratio. A systematic evaluation of color fastness under standardized washing protocols is currently underway.

Supplementary Materials: The following supporting information can be downloaded at the website of this paper posted on Preprints.org, Figure S1: Coloring performance across different combinations of weight ratio and pH. SIP:chitosan weight ratios are (a) 25:1, (b) 5:1, and (c) 2:1; Table S1: Effect of pH on the colorimetric parameters of hair tresses treated with SIP–chitosan mixtures at a fixed weight ratio (SIP:chitosan = 25:1); Table S2: Effect of pH on the colorimetric parameters of hair tresses treated with SIP–chitosan mixtures at a fixed weight ratio (SIP:chitosan = 5:1); Table S3: Effect of pH on the colorimetric parameters of hair tresses treated with SIP–chitosan mixtures at a fixed weight ratio (SIP:chitosan = 2:1).

Author Contributions: Conceptualization, T.M.; methodology, T.M.; software, T.M.; validation, T.M.; formal analysis, T.M.; investigation, T.M.; resources, T.M. and A.N.; data curation, T.M.; writing—original draft preparation, T.M.; writing—review and editing, T.M.; visualization, T.M.; supervision, T.M.; project administration, T.M.; funding acquisition, T.M. All authors have read and agreed to the published version of the manuscript.

Funding: This research was funded by JSPS KAKENHI, Grant Numbers JP23K28281 and JP22K18608. Additional support was provided by Hokkaido SODA Co., Ltd. in the form of a research grant for fundamental research.

Data Availability Statement: The data presented in this study are available from the corresponding author upon reasonable request. The data are not publicly available because they consist of raw experimental measurements generated for this study.

Acknowledgments: The authors thank Dr. Dong-Hwan Shin and Ms. Chikako Inoue for their technical assistance. The authors also acknowledge the NIMS Bioanalysis Facility, and National Institute of Technology, Hakodate College for access to instrumentation and technical support.

Conflicts of Interest: T.M. declares no conflict of interest. A.N. is an employee of Hokkaido SODA Co., Ltd., which provided financial support and chitosan samples for this study. The company had no role in study design; in the collection, analysis, or interpretation of data; in manuscript writing; or in the decision to publish the results.

 doi:10.20944/preprints202603.2517.v1

Abbreviations

The following abbreviations are used in this manuscript:

SIP	size-controlled ink particles
DLS	dynamic light scattering
SEM	scanning electron microscopy
UV-Vis	ultraviolet–visible
DHICA	5,6-dihydroxyindole-2-carboxylic acid
FAO	Food and Agriculture Organization of the United Nations

References

1. Kim, K.; Kabir, E.; Jahan, S. A. The use of personal hair dye and its implications for human health. *Environment International* **2016**, *89-90*, 222-227.
2. Statista Research Department. Global Hair Coloring Market Size 2022 & 2029. Available online: https://www.statista.com/statistics/972997/global-hair-color-market-value/ (accessed on 24 February 2026).
3. Nohynek, G. J.; Fautz, R.; Benech-Kieffer, F.; Toutain, H. Toxicity and Human Health Risk of Hair Dyes. *Food Chem. Toxicol.* **2004**, *42*, 517–543.
4. Mukkanna, K. S.; Stone, N. M.; Ingram, J. R. Para-Phenylenediamine Allergy: Current Perspectives on Diagnosis and Management. *J. Asthma Allergy* **2017**, *10*, 9-15.
5. Tkaczyk, A.; Mitrowska, K.; Posyniak, A. Synthetic organic dyes as contaminants of the aquatic environment and their implications for ecosystems: A review. *Science of The Total Environment* **2020**, *717*, 137222.
6. Cui, H.; Xie, W.; Hua, Z.; Cao, L.; Xiong, Z.; Tang, Y.; Yuan, Z. Recent Advancements in Natural Plant Colorants Used for Hair Dye Applications: A Review. *Molecules* **2022**, *27*, 8062.
7. Kalita, H.; Mohanty, J. P.; Pokhrel, G. Formulation and Evaluation of Natural Herbal Hair Dye Gel Using Lawsonia inermis (Henna Leaves) and Skin Irritation Studies in Albino Rats. *Journal of Pharmacy and Pharmacology* **2022**, *10*, 18-24.
8. Boga, C.; Delpivo, C.; Ballarin, B.; Morigi, M.; Galli, S.; Micheletti, G.; Tozzi, S. Investigation on the dyeing power of some organic natural compounds for a green approach to hair dyeing. *Dyes and Pigments* **2013**, *97*, 9-18.
9. Slominski, A.; Tobin, D. J.; Shibahara, S.; Wortsman, J. Melanin Pigmentation in Mammalian Skin and Its Hormonal Regulation. *Physiological Reviews* **2004**, *84*, 1155–1228.
10. Menichetti, A.; Mordini, D.; Vicenzi, S.; Montalti, M. Melanin for Photoprotection and Hair Coloration in the Emerging Era of Nanocosmetics. *Int. J. Mol. Sci*. **2024**, *25*, 5862.
11. Nguyen, L.; Do, X.; Pham, H.; Duy-Thanh, D.; Than, U.; Nguyen, T.; Nguyen, V.; Le, D.; Nguyen, D.; Kieu, K.; Nguyen, P.; Vu, M.; Tran, N.; Nguyen, T.; Nghiem, L.; Nguyen, T.; Nguyen, N.; Hoang, N. Different Biocompatibility and Radioprotective Activity of Squid Melanin Nanoparticles on Human Stromal Cells. *ACS Omega*. **2024**, *9*, 36926-36938.
12. Solano, F. Melanin and Melanin-Related Polymers as Materials with Biomedical and Biotechnological Applications—Cuttlefish Ink and Mussel Foot Proteins as Inspired Biomolecules. *Int. J. Mol. Sci*. **2017**, *18*, 1561.
13. Brenner, M.; Hearing, V. J. The Protective Role of Melanin Against UV Damage in Human Skin. *Photochem. Photobiol.* **2008**, *84*, 539–549.
14. Meredith, P.; Sarna, T. The Physical and Chemical Properties of Eumelanin. *Pigm. Cell Res.* **2006**, *19*, 572–594.
15. Derby, C. Cephalopod ink: production, chemistry, functions and applications. *Mar Drugs*. **2014**, *12*, 2700-2730.
16. Food and Agriculture Organization of the United Nations (FAO). The State of World Fisheries and Aquaculture 2024: Towards Blue Transformation. FAO **2024**. Available online: https://doi.org/10.4060/cd0683en (accessed on 24 February 2026).

 doi:10.20944/preprints202603.2517.v1

17. Xie, W.; Pakdel, E.; Liu, D.; Sun, L.; Wang, X. Natural Eumelanin and Its Derivatives as Multifunctional Materials for Bioinspired Applications: A Review. *Biomacromolecules* **2019**, *20*, 4312-4331.
18. Matsuura, T.; Hino, M.; Akutagawa, S.; Shimoyama, Y.; Kobayashi, T.; Taya, Y.; Ueno, T. Optical and Paramagnetic Properties of Size-Controlled Ink Particles Isolated from Sepia officinalis. *Biosci. Biotechnol. Biochem*. **2009**, *73*, 2790–2792.
19. Matsuura, T.; Watanabe, S.; Akutagawa, S.; Shimoyama, Y.; Kobayashi, T.; Taya, Y.; Ueno, T. Electron Spin Resonance Spectroscopic Study of Size-Controlled Ink Particles Isolated from *Sepia officinalis*. *Jpn. J. Appl. Phys*. **2010**. *49*, 06GJ11.
20. Matsuura, T.; Shimoyama, Y.; Kobayashi, T.; Taya, Y.; Ueno, T. Paramagnetic Properties of Size-Controlled Squid Ink Particles Dispersed in Water. *Jpn. J. Appl. Phys*. **2011**, *50*, 06GH13.
21. Matsuura, T.; Kato, T.; Minato, K.; Ueno, T. Utilization of Size-Controlled Squid Ink Particles as Enhancer for the Porosity of Titania Electrode in Dye-Sensitized Solar Cell. *Jpn. J. Appl. Phys*. **2012**, *51*, 06FG07.
22. Matsuura, T.; Kato, T.; Horii, M.; Todo, S.; Minato, K.; Ueno, T. Size Estimation of Biological Ink Particles Dispersed in Liquids Using Atomic Force Microscopy. *Jpn. J. Appl. Phys. Conf. Proc*. **2013**, *1*, 011003.
23. Matsuura, T.; Nagai, S.; Ogasawara, K.; Minato, K.; Sakai, M.; Ueno T. Improvement in Performance of Dye-Sensitized Solar Cells with Porous TiO_2 Electrodes Using Squid Ink Particles. *Jpn. J. Appl. Phys*. **2016**, *55*, 06GK01.
24. Micillo, R.; Panzella, L.; Koike, K.; Monfrecola, G.; Napolitano, A.; d'Ischia, M. "Fifty Shades" of Black and Red or How Carboxyl Groups Fine Tune Eumelanin and Pheomelanin Properties. *Int. J. Mol. Sci*. **2016**, *17*, 746.
25. Wortmann, F.J.; Wortmann, G.; Schulze zur Wiesche, E. Spatial Probing of the Properties of the Human Hair Surface Using Wilhelmy Force Profiles. *Langmuir* **2010**, *26*, 7365-7369.
26. Maddar, F.M.; Perry, D.; Brooks, R.; Page, A.; Unwin, P.R. Nanoscale Surface Charge Visualization of Human Hair. *Anal. Chem*. **2019**, *91*, 4632–4639.
27. Mani, I.; Sharma, V.; Tamboli, I.; Raman, G. Interaction of Melanin with Proteins – The Importance of an Acidic Intramelanosomal pH. *Pigment Cell Res*. **2001**, *14*, 170–179.
28. Matsuura, T.; Sugawara, A.; Nishimura, M.; Neichi, T.; Minato, K.; Ueno, T. Surface Modification of Natural Ink Particles for Hair Coloring. *Jpn. J. Appl. Phys*. **2019**, *58*, SIIB02.
29. Rinaudo, M. Chitin and Chitosan: Properties and Applications. *Prog. Polym. Sci.* **2006**, *31*, 603-632.
30. Guzmán, E.; Ortega, F.; Rubio, R. G. Chitosan: A Promising Multifunctional Cosmetic Ingredient for Skin and Hair Care. *Cosmetics* **2022**, *9*, 99.
31. Aranaz, I.; Acosta, N.; Civera, C.; Elorza, B.; Mingo, J.; Castro, C.; Gandía, M. D. L. L.; Caballero, A. H. Cosmetics and Cosmeceutical Applications of Chitin, Chitosan and Their Derivatives. *Polymers* **2018**, *10*, 213.
32. Sionkowska, A.; Kaczmarek, B.; Michalska, M.; Lewandowska, K.; Grabska, S. Preparation and Characterization of Collagen/Chitosan/Hyaluronic Acid Thin Films for Application in Hair Care Cosmetics. *Pure Appl. Chem*. **2017**, *89*, 1829-1839.
33. Ueno, T.; Taya, Y.; Shimono, I. Method for Manufacturing Cuttlefish Ink Pigment Particle. Japan Patent 4605354, **2010**.
34. Morita, T.; Matsuura, T.; Izawa, H.; Kishikawa, K.; Kohri, M. Melanin Upcycling: Creation of Polymeric Materials from Melanin Decomposition Products. *ACS Sustainable Chemistry & Engineering* **2024**, *12*, 7115-7125.
35. Bernsmann, F.; Frisch, B.; Ringwald, C.; Ball, V. Protein adsorption on dopamine-melanin films: role of electrostatic interactions inferred from zeta-potential measurements versus chemisorption. *J. Colloid Interface Sci*. **2010**, *344*, 54-60.
36. Wang, Q. Z.; Chen, X. G.; Liu, N.; Wang, S. X.; Liu, C. S.; Meng, X. H.; Liu, C. G. Protonation constants of chitosan with different molecular weight and degree of deacetylation, *Carbohydrate Polymers* **2006**, *65*, 194–201.
37. Gregory, J.; Barany, S. Adsorption and flocculation by polymers and polymer mixtures. *Adv. Colloid Interface Sci*. **2011**, *169*, 1–12.

 doi:10.20944/preprints202603.2517.v1

38. Szilagyi, I.; Trefalt, G.; Tiraferri, A.; Maroni, P.; Borkovec, M. Polyelectrolyte adsorption, interparticle forces, and colloidal aggregation. *Soft Matter* **2014**, *10*, 2479–2502.
39. Dias, M.F.R.G. Hair Cosmetics: An Overview. *Int. J. Trichology* **2015**, *7*, 2–15.
40. Sargsyan, L.; Hippe, T.; Manneck, H.; Vill, V. Tannin-Mordant Coloration with Matcha (Camelia sinensis) and Iron(II)-Lactate on Human Hair Tresses. *Molecules* **2021**, *26*, 829.
41. Cui, H.; Cai, R.; Hua, Z.; Tang, Y. Plant Colorants for Natural Hair Coloration: Dyeing Optimization and Photostability Assessment. *Sustainable Chem. Pharm*. **2023**, *36*, 101285.